T.3: X-ray spectroscopic studies of plasma produced by intense laser beams

Vipul Arora
Laser Plasma Section
Email: arora@rrcat.gov.in

Abstract

This article describes the study of rapidly evolving hot dense plasma, created by focusing high intensity laser pulses on to solid target surface, carried out at RRCAT, Indore. The basic concept of intense laser matter interaction and x-ray emission from plasma is briefly presented. The study of ionization dynamics of plasma by measuring x-ray yield of different ionic line radiation from the plasma produced by laser pulses from nanoseconds to femtosecond duration is discussed. The experimental signature of radiation transport in plasma is observed from the measurement of x-ray yield in keV spectral region from the mix-Z target. The transient conditions in plasma created by intense ultra-short laser were identified by simultaneous measurements of the inner-shell and the ionic line radiation. The generation and optimization of monochromatic K- x-ray source by intense femtosecond laser pulse were performed. A setup for ultrashort x-ray probe and pump technique developed to study the time resolved x-ray diffraction from a sample undergoing laser generated shock is described. The challenges and future outlook in this field is summarized.

1. Introduction

The recent advent of high peak power laser technology has led to the rapid development of compact laser driven x-ray source. Number of petawatt laser systems are operational or under construction for providing the peak intensity greater than 10^{21} Wcm^{-2} on target to produce the plasma at high density and high temperature emitting intense high energy x-rays to be used in variety of research investigations for potential applications in different branches of applied sciences [1]. The spectral property of x-ray emission is determined by the plasma parameters viz. temperature, density, ionization dynamics, radiation transport. These parameters depend on the physical processes, through which the initial ionization takes place and the dominant mechanism through which laser energy is absorbed in the plasma which in turn is determined by the intensity and the temporal profile of the laser beam. Under optimal conditions, up to 10% of laser energy can be converted into x-ray in > 1 keV spectral range. This makes laser plasmas the most promising high brightness source of x-ray radiation for many scientific and technological applications [2].

X-ray spectroscopic techniques are most widely used to study the dynamics in laser plasma. It is the most suitable technique to study the plasma created with ultra-high intensity, ultra-short laser pulses which is an extreme material state corresponding to solid densities at several electron volt temperature existing for a very short period of time. Moreover, the x-ray radiation emitted from the plasmas produced by ultra-short laser pulses are inherently ultra-short in nature (of the order of the laser pulse duration) and are of potential use in time- resolved x-ray diffraction study.

In this article, we describe the experimental studies of laser plasma x-ray source generated by the interaction of long (3 ns), short (30 ps) and ultra-short (45 fs) laser pulses carried out at RRCAT, Indore. The influence of various laser and target conditions on driven x-ray source for application has been investigated using in house developed x-ray spectrographs. The keV x-ray line emission yield from the magnesium plasma produced by laser pulses of duration extending from nanosecond to femtosecond at constant laser fluence was studied to infer the role of ionization dynamics. The radiation transport in plasma was studied by measuring keV x-ray emission from copper target in the presence of high –Z impurity. The dynamical plasma conditions in ultra-short high intensity laser plasma were studied by simultaneous measurements of the inner-shell and the ionic x-ray line radiation from ultra-short laser-produced magnesium plasma. Subsequently, bright ultra-short Kα- x-ray source between 1 - 8 keV photon energy generated by high intensity femtosecond laser produced plasma was optimized for maximizing photon flux and obtaining narrow spectral width x-ray line radiation. The probe x-ray pulses were used for studying shock wave propagation in silicon crystal under laser excitation.

2. Intense laser matter interaction

Interaction of high power laser with solid generates a hot rapidly evolving plasma which expands outwards to form a monotonically decreasing density profile. The laser light cannot propagate in a region of density higher than the critical density which is the density at which the laser frequency equals the local plasma frequency. The region of plasma upto the critical density (under-dense region) is thus directly heated by absorption of the laser energy. The absorbed laser energy is then transported as heat via thermal conduction and electron transport into the over-dense region beyond the

critical density (where the laser light cannot penetrate) [3]. On the other hand, when an ultra-short laser pulse is incident on a solid target, solid density plasma is generated by the initial part of the pulse. This plasma cannot expand significantly during the laser pulse (due to the very short time involved) and rest of the interaction occurs with the near solid density plasma, The laser energy is absorbed in the plasma by collisional or collision-less mechanisms depending on the focused intensity, the laser pulse duration, and its wavelength. The most important absorption mechanisms in the interaction region typical to short and ultra-short laser produced plasma are inverse bremsstrahlung, resonance absorption, vacuum heating, j x B heating etc. [3]. High density (10^{21} cm^{-3}) plasma heated to a temperature of hundreds of electron volt is an intense source of x-ray radiation.

3. X-ray emission in laser plasma interaction

The overall emission spectrum from laser produced plasma is a superposition of line radiation (bound-bound radiation) on a broad continuum due to free-free and free-bound radiation. The relative yield due to these processes depends on the plasma parameters (n_e, T_e) [4]. Excitation and de-excitation of electrons provides the main mechanism responsible for x-ray emission from a plasma. These take place between bound states, between free and bound states and between the free states. Bound-bound transitions lead to emission of photons with discrete energies determined by the atomic structure of the ion. Free-bound transitions include processes by which a free electron recombines with an ion to one of its bound state. Since the free electron can have any energy, this leads to continuous emission spectrum. Free-free emission is produced by unbound (free) electrons "colliding" with ions through an interaction between the electron charge and the Coulomb field of the ion. Such collisions lead to the continuous acceleration of electrons and the production of bremsstrahlung (free-free) emission radiation. This features a broad range of emitted wavelengths, characteristic of the plasma temperature. The total spectral emission from a plasma has contributions from each of these processes leading to a mixture of discrete lines riding on continuous emission.

The emission in the x-ray region has been widely used for the investigation of laser-plasma interaction mechanisms [2, 5]. The influence of the plasma parameters on the spectral and spatial features of the x-ray emission allows a direct mapping of the laser plasma interaction processes such as partition of energy between thermal and non-thermal electrons [5] in the plasma. Quantitative interpretation of plasma parameters requires the knowledge of the ionization equilibrium at any time and position inside the plasma. This necessitates the solving of both space and time dependent system of rate equations and equations describing the hydrodynamic motion. Furthermore, the radiative transfer problem, involving the absorption and emission of radiation along a propagation path inside the plasma must be included, as it leads to a significant modification in the intensities and profiles of the lines in the emission spectrum. X-ray spectroscopic methods used for diagnostics are based on the interpretation of at least one of the following quantities: spectral line width or profiles, relative continuum intensities, and relative line intensities. The spectral lines that are strongly dependent on one of the plasma parameters but weakly dependent on other parameters have to be identified. For example, electron temperature can be determined from the ratio of the intensities of the resonance lines emitted by the plasma.

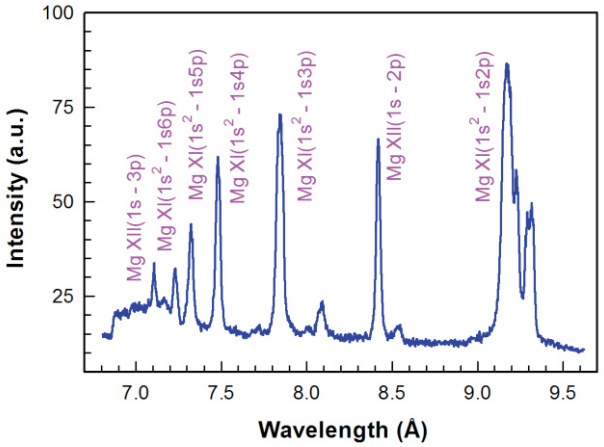

Fig. T.3.1: X-ray spectrum of magnesium plasma produced using nanosecond laser pulses.

A typical high resolution x-ray spectrum of the magnesium plasma [6], generated using a 2 J, 3 ns laser beam, focused to an intensity of ~ 5 x 10^{12} W cm^{-2}, is shown in Figure T.3.1. Various prominent lines in the spectral range of 6.9 Å to 9.6 Å are identified as transitions in He-like (Mg^{+10}) and H-like (Mg^{+11}) magnesium ions. The x-ray emission of energy > 5 keV can be easily obtained from the solid targets irradiated by ultra-short pulse laser of moderate focused intensity (> 10^{17} Wcm^{-2}). Figure T.3.2 shows the typical x-ray spectrum from plasma produced by fs laser pulses [7]. In the spectrum of titanium, both Kα- at 4.5 keV and Kβ- at 4.9 keV can be seen. In the same figure, copper spectrum shows Cu Kα- at 8 keV, and the silicon escape peak at ~6.3 keV (as the silicon Kα- photon energy is 1.74 keV). The Cu Kβ- (8.9 keV) is not seen

here due to its strong attenuation by a Ni filter used in front of the charged coupled device (CCD) used to record the spectrum. Similarly, the characteristics Zn Kα- line at 8.6 keV is seen in the spectrum of zinc.

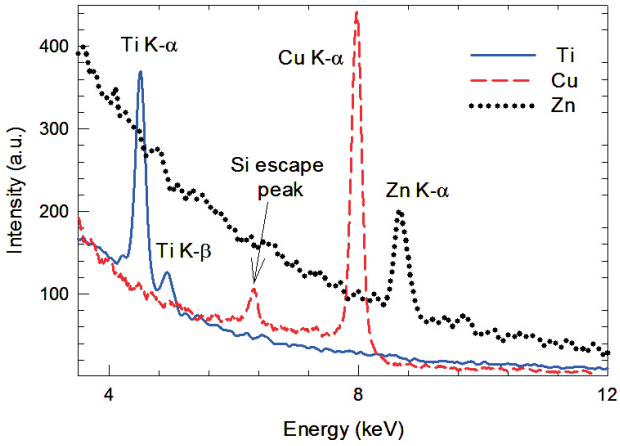

Fig. T.3.2: The Kα- x-ray emission spectra of titanium, copper, zinc from plasma produced by fs laser pulses.

4. Radiation transport in plasma

The radiative properties of laser produced plasma are determined by the hydrodynamic parameters and energy transport. The opacity, as well as the emissivity, of the laser-produced high energy density plasma, heated to a temperature of a few hundreds of eV, is so high for keV emission such that the light emitted from deep inside the plasma is absorbed strongly during propagation through the surrounding plasma. The opacity is the parameter that quantifies how transparent or opaque is the plasma to the radiation. The optical depth, $\tau(\nu)$, is related to the opacity by

$$\tau(\nu) = \kappa(\nu)\rho x,$$

where $\kappa(\nu)$ is the opacity per unit mass (typically measured in units of cm^2 /g), ρ is the density, and x is the optical path length. The opacity is generally a rapidly varying function of frequency. Therefore, the knowledge of the frequency dependent opacity is necessary to obtain high conversion of incident laser energy into x-ray emission. Opacity depends on the plasma temperature, density, and elemental composition [8]. Next, the presence of other element may alter the opacity of the plasma. It is important in applications for example *hohlraum* cavity where mixture of elements like gold and copper are used as ablator wall material to increase the sub-keV x-ray yield.

The experiment for studying radiation transport was carried out by irradiating thick planar foils of gold, copper, and their mix-Z alloys of different atomic compositions, with a frequency-doubled 4 J, 3 ns Nd: glass laser beam focused to an intensity of ~ 10^{13} W cm^{-2}. High resolution x-ray spectrum from the plasma was recorded with an x-ray crystal spectrograph. The x-ray intensity was integrated over the spectral range of 7.8 – 10.9Å for different atomic compositions of Au–Cu mix–Z target. Figure T.3.3 shows that the integrated keV x-ray yield decreases sharply with increase in the fraction of gold in the mix –Z plasma [9]. A reduction factor of ~ 2.1 in the integrated keV x-ray yield is observed for 0.12 Au – 0.88 Cu mix–Z target with respect to pure copper. For the optimum composition for maximum sub-keV conversion (Au 0.43 – Cu 0.57) observed for the same laser irradiation conditions [10], the keV x-ray yield is observed to reduce by a factor of ~ 6.7 compared to that for pure copper.

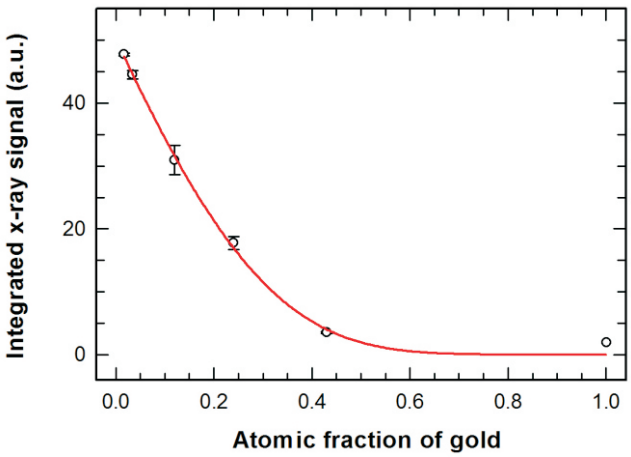

Fig. T.3.3: Variation of the integrated x-ray yield as a function of atomic fraction of gold in the mix-Z target.

The above results on the substantial decrease in the keV x-ray yield in gold–copper mix–Z plasmas can be understood by considering the absorption of the L–shell line emission of copper ions offered by the gold ions present in the mix–Z plasma. In general, the spectral line opacity is given in terms of the optical depth τ_λ as

$$\tau_\lambda = \varphi(\lambda)\int_0^L k_\lambda(x)dx$$

where $\varphi(\lambda)$ is absorption line shape function, k_λ is the absorption coefficient of the plasma at wavelength λ, and L is the path length traversed in the plasma. The transmission of the radiation through the plasma is given by exp $(-\tau_\lambda)$ which depends on the path length traversed and the absorption coefficient. The latter includes both the bound–bound

absorption and the free–bound absorption (opacities). For the temperature and density conditions of the present study, the opacity estimates indicate that gold has a higher free–bound opacity in the spectral region of the L-shell emission of the copper ions. The absorption of the copper L-shell line radiation in gold ions decreases the emission intensity of these lines from the mix–Z plasma containing gold ions. The electron vacancy in the gold ions created due to bound–free transition on absorption of copper L-shell line radiation is subsequently filled through a cascade of radiative transitions of electrons from the higher energy levels. This leads to the emission of radiation at a longer wavelength compared to the copper L-shell line wavelength. Since many such transitions are possible due to multiple N- and O-shells in gold ions, the emitted radiation occurs at different wavelengths in the sub-keV region. Thus, a fraction of the copper L-shell keV line radiation of the gold–copper mix–Z plasma reappears as enhanced sub-keV x-ray emission.

5. Ionization dynamics

Investigation of the H-like and He-like transition lines and their dielectronic satellites emitted during the laser pulse can give direct knowledge of ionization dynamics of rapidly evolving hot and dense plasmas. The x-ray emission properties of dense plasmas in non-local thermodynamic equilibrium, when ionization dynamics is expected to depart more from the steady-state regime, will be different. A comparison of relative fraction of ionization state for widely different laser pulse duration can give estimation of timescale of ionization in the plasma. We have carried out a systematic study of the keV x-ray line emission from the plasmas produced by laser pulses of femtosecond, picosecond, and nanosecond duration [11]. The laser pulse duration governs the hydrodynamics of the plasma produced on the target and its role becomes critical in the transient regimes of plasma formation, when the x-ray emission takes place from the plasma regions characterized by rapid changes and strong spatial gradients of hydrodynamic quantities.

In Figure T.3.4, the relative x-ray yields for different line radiations namely Mg XI $1s^2$– 1s 2p (He-α), Mg XI $1s^2$ – 1s 3p (He-β), Mg XII 1s –2p (H-α) and Mg XII 1s –3p (H-β) lines are shown for different pulse durations used in the experiment. The x-ray emission from the H-like ions from the femtosecond laser plasma generated at higher intensity is absent and a relatively weak emission is observed from the H-like ions in the picosecond laser produced plasma at lower intensity. It indicates that the ionization to highly ionized species from the low ionized species, which requires much longer time, does not take place during the laser pulse if the former is longer than the latter. If we compare the x-ray emission from the plasma produced by ns laser pulse at a much lower intensity, where steady state is reached, the intensity of the Hα- line emission is much stronger. The fact that the Hα- line is much weaker from the ps laser produced plasma shows that during the ps laser pulse, steady state is not reached and hence there is a substantial departure of ionization dynamics from the equilibrium regime. This can happen if the pulse duration is much shorter than the time required to reach ionization equilibrium between He-like and H-like ions. The ionization equilibrium time [11] was calculated by solving the rate equations for collisional ionization, three-body recombination, and radiative recombination processes.

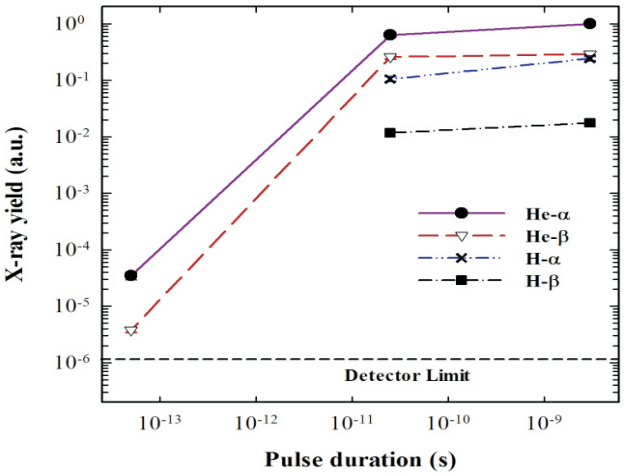

Fig. T.3.4: The relative conversion efficiency of the magnesium He-α, He-β, H-α and H-β lines for the three different pulse durations.

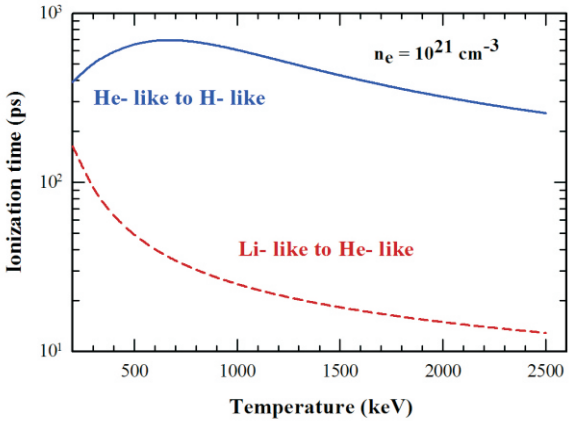

Fig. T.3.5: Ionization equilibrium time calculated for ionization of He-like magnesium ions to H-like ions for different values of T_e at a fixed value of n_e of 10^{21} cm^{-3}. The dashed curve is for ionization of Li-like magnesium ions to He-like ions.

Figure T.3.5 shows the time required for the ionization of the He-like magnesium ions to H-like ions, and for the Li-like magnesium ion to He-like ions, for different values of the electron temperature up to 2.5 keV, for a fixed value of electron density of 10^{21} cm^{-3} (the critical density for 1054 nm). For instance, the ionization equilibrium time between the Li-like ions and the He-like ions, and between the He-like ions and the H-like ions at the electron temperature of 2.4 keV are calculated to be 15 ps and 250 ps respectively. This explains the complete lack of line emission from H-like ions and negligible emission from He-like ions in the spectrum recorded with 50 fs laser pulses. However, as the plasma expands after the laser pulse is over, it undergoes evolution of density and temperature in the expanding plasma. During certain period of expansion the temperature may remain high enough to produce high ionization states of Mg^{11+} and Mg^{10+} provided the ionization equilibrium time is smaller than the plasma expansion time scale.

6. X-ray emission in ultra-short laser pulse interaction

X-ray spectroscopy of dense plasma produced by high intensity ultra-short laser provides information for the basic research and optimization of plasma parameters for controlling x-ray source properties for applications. We studied the keV x-ray emission spectrum (Figure T.3.6) from magnesium plasma produced by the 45 fs duration laser pulses, focussed at an intensity of 4 x 10^{17} W cm^{-2} [12]. It has well defined ionic x-ray line features corresponding to high temperature plasma, as well as characteristic K-α emission from cold atom and lower charge ions.

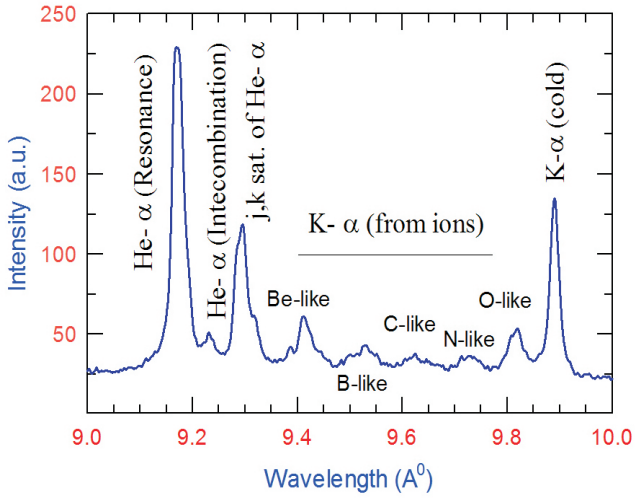

Fig. T.3.6: High resolution x-ray spectrum of magnesium plasma produced by 45 fs duration laser pulses focussed at an intensity of 4x10^{17} W cm^{-2}.

The spectrum is different from that produced by long ns duration laser pulses. The identified lines are He–α resonance transition Mg XI $1s^2\ ^1S_0 - 1s\ 2p\ ^1P_1$ at = 9.17 Å, weak He–α intercombination transition (IC) Mg XI$1s^2\ ^1S_0 - 1s\ 2p\ ^3P_{1,2}$ at =λ 9.23 Å blended with the s, t, m, n satellite lines, the group of q, r and j, k dielectronic satellite lines of the Li-like transitions at λ = 9.32 Å, and the K-α emission from un-ionized Mg atoms at 9.87 Å. The q, r and j, k satellites lines are not well resolved due to the degraded spectral resolution on account of the source size broadening, but are well resolved from the IC line. A relatively lower intensity shifted K-α emission, from Be-like, B-like, C-like, N-like, and O-like Mg ions, is also observed on the lower wavelength side of the K-α emission from the Mg atoms. The K-α line excitation is by the hot electrons which are generated through collective mechanisms. These electrons, on penetration into the cold target material, generate continuum hard x-ray bremsstrahlung and the characteristic K-α line radiation. Simultaneous presence of the K-α lines from un-ionized atoms as well as the satellite K-α lines from Be- to O-like ions, is due to the presence of pre-plasma. The satellite lines are inner-shell K-α transitions induced by the hot electrons in lower charged ionic species present in the initial low temperature pre-pulse plasma [13].

The observed x-ray spectrum corresponds to the time and space averaged values of density and temperature of the plasma undergoing rapid hydrodynamic evolution. Spectroscopic analysis and modelling of x-ray spectrum was carried out using the single cell spectral analysis code PrismSPECT [14]. It generates K-shell emission spectra based on time-dependent solution of rate equations considering non-local thermodynamic equilibrium. Least-squares comparison of normalized PrismSPECT spectrum with the experimentally observed spectrum was carried out. A fit for ionic line emission with temperature T_e = 130 eV, and electron density $n_e \sim 5.4 \times 10^{20}$ cm^{-3}, T_{hot} = 50 keV and the hot electron fraction = 0.01 was obtained. A spatially and temporally averaged value of the electron temperature of ~100 -200 eV and a hot electron fraction of ~ 0.01 is expected in our experimental conditions [12]. The electron density value which fits the spectra is close to the turning point density (~ 7.8×10^{20} cm^{-3}) for a 45° obliquely incident 800 nm Ti:sapphire laser beam.

7. Bright monochromatic ultra-short K-α x-ray source

Improvement of the conversion of the laser energy to the energy of K-α radiation can be achieved by increasing the hot electron number and temperature [15]. However, the logarithmic growth of the cross-section for the K-α photon

emission for relativistic electron energies in a thick target does not entail an increase in the conversion. The maximum K-α yield occurs for an optimal T_{hot} of 3-6 times the K-α energy [16]. Further, the x-ray radiation up to the K-α photon absorption length can be collected from the target. Thus the laser irradiation conditions have to be optimized for controlling the electron energies. The laser pulse duration is the effective way to optimize laser intensity for maximizing x-ray yield. The x-ray yield of the titanium, iron and copper K-α radiation was optimized with laser pulse duration for a constant fluence of 3.8 x 10^4 J cm^{-2}. K-α The optimal pulse duration for maximum K-α intensity for Ti, Fe, Cu is (420±90) fs, (325±75) fs, (250±50) fs respectively [17]. At the optimal pulse duration, it is expected that the hot electron temperature is optimum and x-ray source is located close to the surface and does not get reabsorbed. The highest conversion efficiency of 3.2x10^{-5} and 2.7 x 10^{-5} is estimated for Ti and Fe K-α.

It has been discussed earlier that ultra-short laser interaction with solids produces plasma with bi-Maxwellian electron energy distribution function with bulk temperature and hot electron temperature. Increasing the bulk temperature leads to the generation of K-α radiation from ions which are blue shifted and broadens the K-α lines [13]. It is to be noted that the narrow bandwidth probe radiations are desirable in time resolved x-ray diffraction setup to obtain better angular resolution which increases the sensitivity of the detection [13]. The contribution of this factor in the overall temporal resolution becomes important when the extent of modification of the diffracted signal is rather small.

Alternatively, broadening may also be due to the ions present in the long-scale length plasma produced in front of the target by pre-pulse. It is well known that ultra-short pulse laser systems based on chirped pulse amplification are invariably associated with an ASE pre-pulse prior to the main pulse. The pre-plasma formed by the pre-pulse expands before the arrival of the main laser pulse. In our experiment, the pre-pulse intensity was ~ 10^{11} W cm^{-2}, which can produce plasma of few tens of eV temperature, with multiply charged titanium ions. The inner-shell transition in these ions will be shifted more towards high energy side and eventually their blending with the transition in cold atom would increase the line bandwidth. It may be noted that the appearance of strong inner-shell transitions from ionized atoms will lead to an increase in the integrated inner-shell x-ray conversion efficiency. ASE intensity increases with the laser fluence. To clearly bring out the role of preplasma, the inner-shell x-ray emission spectra for two different laser fluences of 3.5 x 10^3 J cm^{-2} (45 fs) and 4.2 x 10^4 J cm^{-2} (600 fs), at a fixed laser intensity of ~ (7.4 ± 0.4) x 10^{16} W cm^{-2} was recorded (Figure T.3.7). The spectral width of the K-α_1 component for the smaller laser fluence 4.2 eV, which is much smaller in comparison to the spectral width of ~ 9.1 eV, observed for the higher laser fluence. These observations indicate that the spectral width of the K- radiation is closely linked to the laser fluence rather than the laser intensity and therefore pre pulse has to be controlled for obtaining narrow bandwidth x-ray radiation.

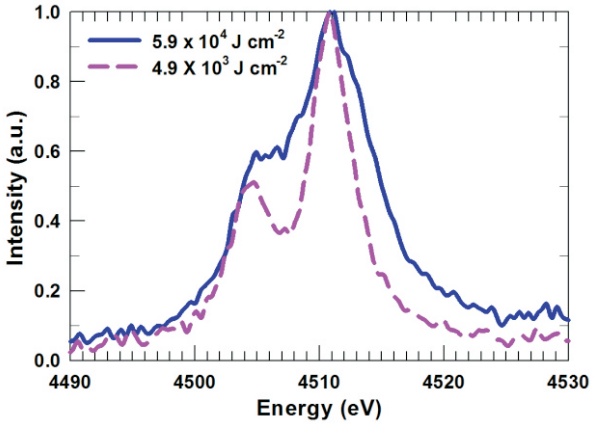

Fig. T.3.7: Normalized K- line radiation profile at two different laser fluences.

8. Time resolved x-ray diffraction

X-rays emitted from ultra-short laser produced plasmas have been used to study the structural dynamics of a wide range of samples from a single crystal to polycrystalline materials. The time resolved studies are performed in pump-probe scheme where an optical pump (laser) deposits its energy in the sample to modify the lattice. This causes changes in the electron distribution function leading to changes in the atomic interaction potential so that the matter loses crystalline order and becomes molten on a sub-ps time scale. The melting can be seen by observing a large decrease of the integrated intensity of the Bragg-reflections.

A typical pump-probe setup [18] with laser produced plasma x-ray source, used at the RRCAT, Indore, is shown in Figure T.3.8(a). The pump pulse consists of a 300 ps laser pulse which is used to modify the lattice structure of the crystalline sample. This pulse is a small fraction of the laser pulse which produces x-rays, which are used as the ultra-short probe. With a variable delay line, the x-ray probe is made to diffract from the perturbed structure at different times after the crystalline lattice is distorted. The x-ray diffraction profile changes as the distance between atomic planes changes, leading to the change in angle for Bragg reflection. The line shape and position of the reflected line radiation indicate the state of the lattice as transient effects pass through the penetration depth

of x-rays. In these experiments, inhomogeneous spacing and lattice expansion are observed. The transient dynamics in the material is resolved by analyzing the shift or broadening of the diffraction signal as shown in Figure T.3.8(b).

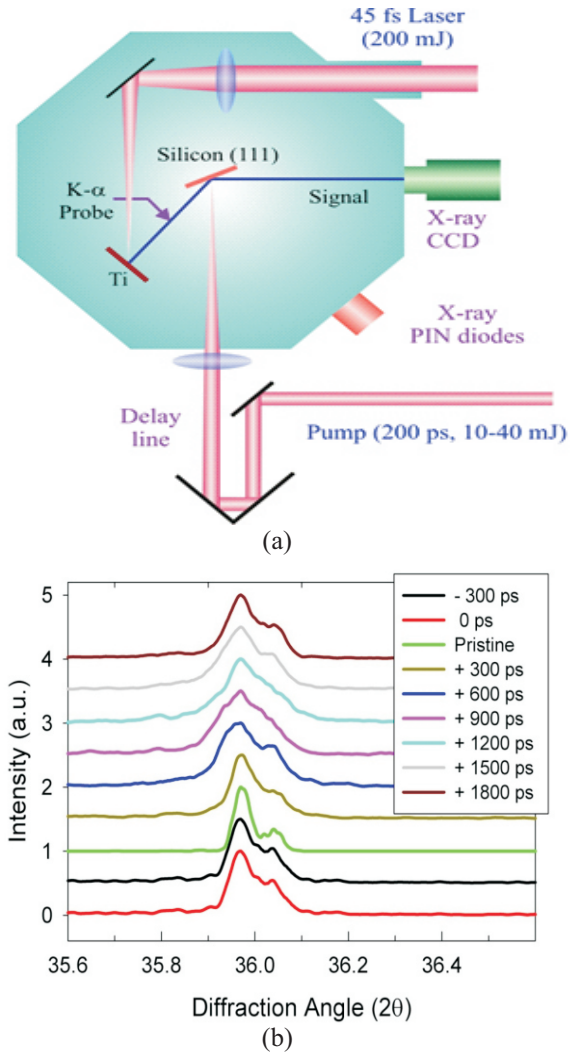

Fig. T.3.8: (a) Experimental setup, (b) variation of the FWHM of the Fe K-α_1 line radiation as function of the delay.

The diffraction profiles of Fe $K_{\alpha 1}$ (6403.8 eV) and $K_{\alpha 2}$ (6390.8 eV) are well resolved for zero (and negative) delays. It is observed that the diffraction pattern broadens with increasing the time delay up to +1200 ps. After that, the broadening reduces and finally comes back to the original state for delays larger than +1500 ps. It may be noted that the broadening of the diffracted signals is predominantly towards higher angles, which indicates lattice compression induced by the pump laser beam. The small spreads towards lower angles also appear after 300 ps implying lattice expansion. It is the signature of thermal disordering effect due to heating, indicating a larger role of a thermal wave. The modification of the lattice is either due to the laser ablation of very thin surface of the silicon or due to the stress caused at the front of thermal expansion due to the surface energy deposition. The ablation occurs when the laser fluence is above the threshold of ionization of the ablation vapour and rate of ablation depends on the laser fluence. The pressure wave intensity would decrease monotonically as it propagates in the sample. The lattice change observed is manifested as a modification in x-ray diffraction profile integrated over the penetration depth for that photon energy. By the time the rocking curve is first recorded (the zero time) the shock wave would have penetrated by about 2 μm. However, this will not affect the measurements because the penetration depth of the Fe K-α x-rays in Si (111) is 11.3 μm, which is much larger than 2 μm. The observed maximum compression is 0.4%, which corresponds to a pressure of 0.8 GPa (8 kbar). A study of the time evolution of the rocking curve can be an effective way to understand the propagation of the shock waves inside the crystal. From the penetration depth of Fe K-α at 6.4 keV in Si, it can be calculated that the shock wave propagates with a speed of 9.7×10^5 cm/s.

9. Summary and future outlook

The experimental study of the x-ray emission from plasma produced by laser pulses from nanosecond to femtosecond duration was described. The study was aimed to develop conditions for high conversion efficiency of laser energy into monochromatic x-ray line radiation for its application as an x-ray probe for time resolved measurements. It has been shown that x-ray emission depends on the ionization dynamics and opacity of the plasma. The dynamical conditions prevalent in ultra-short laser produced plasma have been identified by simultaneous measurement of ionic and inner shell x-ray line radiation. The K-α x-ray source between 1–8 keV was optimized for maximum conversion efficiency and narrow bandwidth line radiation. The results of optimal laser pulse duration for the maximization of x-ray intensity have been explained in terms of efficient generation of optimal energy hot electrons due to the trade-off between the electron energy and re-absorption of the emitted radiation in coming out of the target. The reason for the spectral broadening is attributed to the inner-shell transitions in multiply-charged ions in the pre-plasma. The dynamics of the strain propagation has been inferred by monitoring the evolution of the rocking curve width of the shocked sample at different time delays between the pump and the probe pulse.

The results presented are an important basis for future research relevant to inertial confinement fusion and material science. For instance, x-ray probe of energy 10 keV is required for probing density (10^{26} cm^{-3}) of the compressed matter. More data on x-ray scaling of x-ray photon yield with laser energy at higher photon energies are required with more powerful lasers (> 100 TW) such as recently installed 150 TW and upcoming 1 PW laser facilities at RRCAT. There is upsurge in interest for the investigation of warm dense matter state isochroically heated by proton beams with a pump probe technique. The spectrally narrow high energy x-ray probes are desirable in x-ray scattering or diffraction techniques. Such experiment requires the x-ray source with high photon flux and high sensitivity x-ray detectors. Next, the high resolution spectral measurement can be used for the quantitative estimation of the heating induced by the proton beam in the target. Future work will aim to achieve the sub-picosecond temporal resolution to investigate the strain and lattice dynamics in photo-excited samples.

Acknowledgment

This work is a part of the Ph. D. thesis of the author, which was carried out under the guidance of Dr. P. D. Gupta, former Director, RRCAT Indore and Dr. P. A. Naik, Director, RRCAT Indore. The author is grateful for their valuable guidance and encouragement. The author is also thankful to Dr. J. A. Chakera, Head, Laser Plasma Section and colleagues for their help during the work.

References

[1] C. Danson, D. Hillier, N. Hopps, and D. Neely, “Petawatt class lasers worldwide” High Power Laser Science and Engineering, vol. 3, pp. 1-14, 2015.

[2] I. C. E. Turcu, and J. B. Dance, X-rays from laser plasmas: generation and applications, Wiley, New York 1999

[3] W. L. Kruer, The physics of laser plasma interactions, Addison-Wesley, New York, 1988.

[4] H. R. Griem, Principles of plasma spectroscopy, Cambridge University Press, Cambridge, 1997.

[5] D. Giulietti, and L. A. Gizzi, 'X-ray emission from laser-produced plasmas, La Rivista del Nuovo Cimento, vol. 21, pp.1-93, 1998.

[6] V. Arora, S. R. Kumbhare, P. A. Naik, and P. D. Gupta, 'A simple high-resolution on-line x-ray imaging crystal spectrograph for laser–plasma interaction studies', Review of Scientific Instruments, vol. 71, pp. 2644-2650, 2000.

[7] V. Arora *et al.*, “Dispersion-less spectrograph for absolute measurement of multi keV X-ray flux from high intensity laser produced plasmas”, J. Instrum., vol. 8, pp. 010101 -13, 2013.

[8] J. E. Bailey *et al.*, “Experimental investigation of opacity models for stellar interior, inertial fusion, and high energy density plasmas” Physics of Plasmas, vol. 16, pp. 058101-16 (2009).

[9] V. Arora *et al.*, "Effect of gold on keV x-ray emission yield from laser produced plasma of gold-copper mix-Z targets", J. Appl. Phys., vol. 100, pp. 0333061-4 (2006).

[10] J. A. Chakera, *et al.*, 'Dependence of soft x-ray conversion on atomic composition in laser produced plasma of gold–copper mix-Z targets' Applied Physics Letters, vol. 83, pp. 27-29, 2003.

[11] V. Arora, P. A. Naik, B. S. Rao, and P. D. Gupta, 'A comparative study of the ionic keV x-ray line emission from plasma produced by the femtosecond, picosecond and nanosecond duration laser pulses', *Pramana*, vol. 78, pp. 277-288, 2012.

[12] V. Arora *et al.*, “A comparative study of the inner-shell and the ionic line radiation from ultra-short laser-produced magnesium plasma”, Phys. Scr., vol. 89, pp. 115601-9, 2014.

[13] V. Arora, H. Singhal, P. A. Naik, and P. D Gupta, "Conversion efficiency and spectral broadening of the K-α line emitted from planar titanium targets irradiated with ultra-short laser pulses of high intensity", J. App. Phys., vol. 110, pp. 0833051-7, 2011.

[14] Prism Computational Sciences, Madison, WI 53711, U.S.A. (2017).

[15] U. Chakravarty *et al.,* "X-ray enhancement in a nanohole target irradiated by intense ultra-short laser pulses", J. Appl. Phys., vol. 109, pp. 053301-07, 2011.

[16] Ch. Reich, P. Gibbon, I. Uschmann, and E. Forster, "Yield optimization and time structure of femtosecond laser plasma Kα sources", Phys. Rev. Lett., vol. 84, pp. 4846 -4849, 2000.

[17] V. Arora *et al.*, Study of 1–8 keV K-α x-ray emission from high intensity femtosecond laser produced plasma. AIP Adv., vol. 4, pp. 047106-11, 2014.

[18] V. Arora *et al.*, “Study of strain propagation in laser irradiated silicon crystal by time-resolved diffraction of K-α x-ray probe of different photon energies” J. Appl. Phys., vol. 114, pp. 023302 - 5 (2013).